HTML ABSTRACT + LINKS

Strain dependence of lasing mechanisms in ZnO epilayers

H. D. Li, S. F. Yu,[a] A. P. Abiyasa, Clement Yuen, S. P. Lau,
H. Y. Yang, and Eunice S. P. Leong
School of Electrical & Electronic Engineering, Nanyang Technological University, Block S2, Nanyang Avenue, Singapore 639798

(Received 7 February 2005; accepted 19 May 2005; published online 23 June 2005)

The lasing characteristics of highly disordered ZnO thin films deposited on SiO_2/Si substrates with and without a MgO buffer layer have been investigated. We observed that the emission spectra of the ZnO epilayers with and without a MgO buffer are associated with the radiative recombination of free-exciton (~380 nm) and electron-hole plasma (~395 nm), respectively. The difference in the lasing wavelength is due to the induced compressive (tensile) strain along the *c* axis of the ZnO epilayers as a result of the presence (absence) of the MgO buffer layer. It is demonstrated that the strain-induced variation of Mott density inside the ZnO epilayers is responsible for the observed lasing characteristics. © *2005 American Institute of Physics*. [DOI: 10.1063/1.1968418]

The large bandgap and high binding energy of excitons make ZnO a promising material to fabricate high-performance ultraviolet light-emitting devices. Room-temperature (RT) stimulated emission has been demonstrated from optical excitation of ZnO polycrystalline thin films.[1–4] Radiative recombination due to exciton-exciton scattering (EES) at ~390 nm and electron-hole plasma (EHP) at ~395 nm can be observed from ZnO thin films that have undergone different fabrication processes.[1,2,4] Free-exciton (FE) radiative recombination at ~380 nm has also been reported in ZnO microclusters (agglomerated by 50 nm nanocrystallites)[5] and nanowires.[6] However, it has yet to be explained how the different mechanisms of radiative recombination can occur in ZnO thin films and nanostructures. It must be noted that the understanding of radiative recombination mechanisms is essential for the design of high-performance ZnO-based optoelectronics devices. In this letter, we report the strain in highly disordered ZnO epilayers, which can be obtained by thermal annealing of ZnO films deposited on Si substrate with different buffer layers, is responsible for FE and EHP radiative recombinations. The strain dependence of Mott density[7] is attributed to the variation of lasing wavelengths under optical excitation at RT.

ZnO epilayers were deposited on Si (100) substrate with a ~400 nm thick SiO_2 layer by the filtered cathodic vacuum arc (FCVA) technique.[4] During the deposition, the substrate temperature and chamber pressure were set to 230 °C and 9×10^{-4} Torr, respectively. Two types of samples were fabricated: the epilayer structure of sample *a* is ZnO (100 nm)/SiO_2 (400 nm)/Si (substrate) and that of sample *b* is ZnO (100 nm)/MgO (200 nm)/ZnO (100 nm)/SiO_2 (400 nm)/Si (substrate). In these samples, the top 100 nm ZnO thin layer with (002) orientation acts as the active layer to provide radiative recombination. In sample *a*, the 400 nm SiO_2 film acts as the buffer layer to allow the transverse confinement of light into the active layer. Similarly, the MgO (200 nm) film in sample *b* also acts as the buffer layer. The bottom 100 nm ZnO layer in sample *b* allows the deposition of high-quality MgO (200) film by the FCVA technique. These as-grown samples were then annealed in open air (900 °C, 2 h) in a standard Lindberg-type furnace using a quartz tube reactor. Hence, highly disordered ZnO (100 nm) films with strain can be formed to sustain random laser action.[3,4] The optical characteristics of these samples were studied under optical excitation by a frequency-tripled Nd:YAG laser (at 355 nm) at pulsed operation (6 ns, 10 Hz). The optical pump was focused using a cylindrical lens to a stripe of length 5 mm and width 50 μm on the sample surface. The laser emission was measured from the edge of the samples.

Figure 1 shows the lasing spectra and light-light curves of samples *a* and *b*. Based on the samples' structure and random laser theory,[3–5] the lasing phenomena observed from both samples are due to random laser action. Figure 1(a) shows the lasing characteristics of sample *a* with threshold $P_{th}\sim400$ kW/cm^2 and lasing peaks around 391 nm. This is due to EES and EHP radiative recombination. At higher excitation intensities above the threshold, more sharp peaks are excited and EHP is dominant over the lasing spectrum with a peak wavelength at ~395 nm. Furthermore, the increase in pump intensity redshifts the emission peak to ~400 nm. These lasing characteristics are similar to the previous reports on the ZnO films grown on SiO_2/Si (see Ref. 4) and sapphire substrates.[1,2] Figure 1(b) shows the lasing charac-

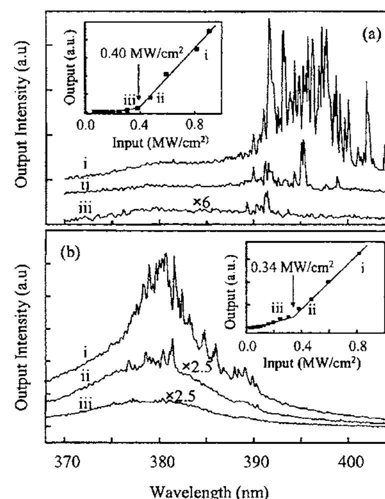

FIG. 1. Emission spectra of the ZnO films (a) without and (b) with the MgO buffer. The insets are the light-light curves.

[a]Author to whom correspondence should be addressed; electronic mail: esfyu@ntu.edu.sg

 © 2005 American Institute of Physics
Downloaded 24 Jun 2005 to 155.69.4.4. Redistribution subject to AIP license or copyright, see http://apl.aip.org/apl/copyright.jsp

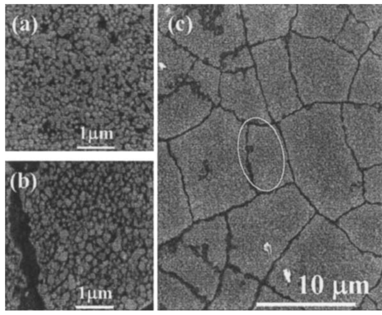

FIG. 2. Scanning electron microscope images of ZnO films (a) without and (b) with the MgO buffer layer. (c) Birds-eye view of (b).

teristics of sample *b* with a threshold $P_{th} \sim 340\ \text{kW/cm}^2$. We observed that the lasing peaks emerge at ~380 nm, which is close to the expected energy level of FE radiative recombination in ZnO at RT.[2] At high pump intensities, FE radiative recombination is still dominant in the lasing spectra. This is because the exciton density is clamped at the threshold due to the lasing mechanism and the triggering of EHP radiative recombination is suppressed.

The difference in lasing wavelength between samples *a* and *b* can be attributed to strain (i.e., mismatch in lattice constant and different degrees of thermal expansion between the active and buffer layers) induced variation of radiative recombination process in ZnO films. We rule out the possibility that the variation of lasing wavelength is due to the difference in size distribution of random cavities in both samples. This is because, from the scanning electron microscopy images as given in Figs. 2(a) and 2(b), it is observed that the size distribution of ZnO irregular grains for both samples is similar (i.e., mean diameter of ZnO grains is ~150 nm). This indicates that the scattering mean free path of ZnO random cavities of both samples generated by thermal annealing is similar. This is evidenced by the coherent backscattering experiment.

In Fig. 2(c), a typical mud-cracking pattern appears in sample *b*, which implies that the sample is under biaxial in-plane tension.[8] From the measured (0002) diffraction peak of x-ray diffraction spectra (not shown), the lattice constants *c* of samples *a* and *b* are estimated to be 0.5250 and 0.5184 nm, respectively. The strain along the *c* axis of the films perpendicular to the substrate is defined by $\varepsilon_{zz}=(c-c_0)/c_0$ (%), where c_0 (~0.5205 nm) is the lattice constant in the unstrained crystal. ε_{zz} for samples *a* and *b* are estimated to be 0.9% and −0.4%, respectively. Hence, it is shown that sample *a* is in tensile strain and sample *b* is in compressive strain.

It must be noted that the resonance energy of excitons in strained ZnO films normally blueshifts with the increase of ε_{zz} (from compressive to tensile strain),[9] but the lasing peaks from our sample with tensile strain are redshifted. Furthermore, the difference in resonance energy of excitons (observed from the spontaneous emission spectra) between the samples *a* and *b* is ~10 meV, which is smaller than that reported in Ref. 9 (i.e., ~20 to ~30 meV). Therefore, the change in lasing wavelength of our samples cannot be attributed to the strain-induced change of exciton energies and the large difference in lasing energy (i.e., ~120 meV) between samples *a* and *b* is due to the change of radiative recombination process.

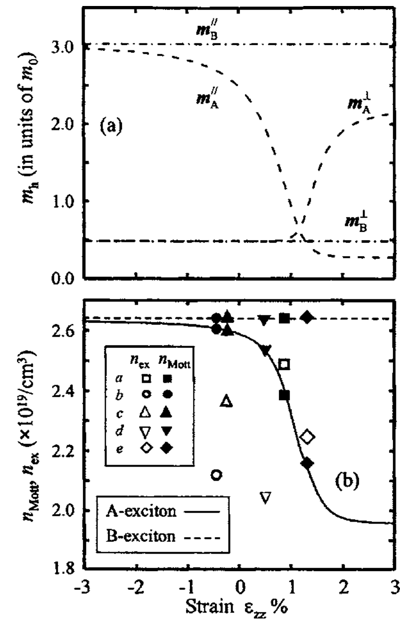

FIG. 3. The strain ϵ_{zz} dependence of (a) the effective hole mass, m_h, and (b) the Mott density n_{Mott} of the *A*- and *B*-excitons in strained ZnO film. The estimated values of exciton density n_{ex} for different samples *a*, *b*, *c*, *d*, and *e* are also shown in (b).

It is known that ε_{zz} can vary the effective mass of holes, $m_h^{\parallel,\perp}$ (∥ and ⊥ denote the directions parallel and perpendicular to the *c* axis, respectively) and thus, the reduced mass m_r, as delineated in the equation $1/m_r^{\parallel,\perp}=1/m_e^{\parallel,\perp}+1/m_h^{\parallel,\perp}$, where $m_e^{\parallel,\perp}$ is the effective mass of electron. The change in ε_{zz} affects the mechanism of radiative recombination as the Mott density n_{Mott} depends on ε_{zz}.[10] Therefore, we investigate the strain dependence of the lasing characteristics of the ZnO films on the effective hole mass of different excitons (i.e., *A*-exciton of Γ_7 band and *B*-exciton of Γ_9 band). In the calculation, *C*-exciton is not considered, as the corresponding oscillator strength is normally weak at RT. The effective hole mass of *A*- and *B*-excitons (i.e., $m_A^{\parallel,\perp}$ and $m_B^{\parallel,\perp}$), can be expressed as[11]

$$\frac{m_0}{m_A^{\parallel,\perp}}=A_{1,2}+\frac{1}{2}A_{3,4}+\frac{1}{4}\left[\left(\Delta_1-\Delta_2^{\parallel,\perp}+\left(D_3-\frac{C_{33}}{C_{13}}D_4\right)\varepsilon_{ZZ}\right)^2+2\Delta_2^{\parallel,\perp 2}\right]^{1/2}\left[\Delta_1-\Delta_2^{\parallel,\perp}+\left(D_3-\frac{C_{33}}{C_{13}}D_4\right)\varepsilon_{ZZ}\right]A_{3,4}, \quad (1)$$

$$\frac{m_0}{m_B^{\parallel,\perp}}=A_{1,2}+A_{3,4}, \quad (2)$$

where m_0 is the free-electron mass, A_{1-4} are the Luttinger parameters, C_{ij} are the components of the elastic stiffness constant, $\Delta_{1,2}$ is the crystal-field splitting energy, and D_{1-4} are the deformation potential constants.[12] It should be noted that the indices *A* and *B* in all expressions given in Ref. 11 for GaN are inverted when applied to ZnO due to the inverse order of the upper Γ_7 and Γ_9 subbands.[13] Figure 3(a) plots $m_A^{\parallel,\perp}$ and $m_B^{\parallel,\perp}$ versus ε_{zz}. It is shown that $m_A^{\parallel,\perp}$ has a strong correlation with ε_{zz}, while $m_B^{\parallel,\perp}$ is independent of ε_{zz}. Our calculated values of $m_{A,B}^{\parallel,\perp}$ for the case of strain-free ZnO materials match well with those given in Ref. 13. The Mott density n_{Mott} can be calculated from $n_{Mott}=m_r^2e^2k_BT/4\pi\hbar^4\varepsilon_r\varepsilon_0$,[10] where the anisotropy of the dielectric constant ε_r, and effective mass, m_r, are replaced by $(\varepsilon_r^{\parallel}\varepsilon_r^{\perp})^{1/2}$

Downloaded 24 Jun 2005 to 155.69.4.4. Redistribution subject to AIP license or copyright, see http://apl.aip.org/apl/copyright.jsp

and $(m_r^{\perp} m_r^{\parallel})^{1/2}$, respectively. Figure 3(b) plots n_{Mott} versus ε_{zz} for *A*- and *B*-excitons. It is noted that the n_{Mott} value for the *B*-exciton ($\sim 2.63\times 10^{19}/\mathrm{cm}^3$) is independent of ε_{zz}. For the *A*-exciton, the n_{Mott} value is large for $\varepsilon_{zz}\leqslant 0$ (i.e., compressive strain) and extends to the maximum value of $2.62\times 10^{19}/\mathrm{cm}^3$ with the decrease in ε_{zz}. However, n_{Mott} decreases abruptly with the increase in ε_{zz} (i.e., tensile strain) and it reduces to $1.95\times 10^{19}/\mathrm{cm}^3$ for $\varepsilon_{zz} > 3\%$.

From our experiment, it is estimated that samples *a* and *b* have ε_{zz} equal to 0.9% and −0.4%, respectively. From Fig. 3(b), the values of n_{Mott} of the *A*-exciton for samples *a* (■) and *b* (●) are found to be $\sim 2.39\times 10^{19}/\mathrm{cm}^3$ and $\sim 2.60\times 10^{19}/\mathrm{cm}^3$, respectively. The excited exciton density n_{ex}, of samples *a* and *b* at threshold can be estimated by using the rate equation $\eta\lambda P_{\mathrm{th}}/dhc \approx n_{\mathrm{ex}}/\tau_{\mathrm{FE}}$, where P_{th} is the pump threshold, λ (=355 nm) is the pump wavelength, *h* is the Planck's constant, *c* is the velocity of light in vacuum, *d* (∼100 nm) is the thickness of active layer, τ_{FE} (∼0.8 ns) is the radiative lifetime of free exciton at RT,[14] and η (∼0.435) is the coupling efficiency. η is deduced by assuming only 87% of light is transmitted into the film and at most 50% of pump intensity is converted into optical gain. It is found that the value of n_{ex} for sample *a* is $\sim 2.49\times 10^{19}/\mathrm{cm}^3$ [i.e., □ in Fig. 3(b)], which is higher than the calculated n_{Mott} of the *A*-exciton in the same sample. This implies that the density of photoexcited excitons can easily exceed the relatively low n_{Mott} value for the *A*-exciton, and hence part of the excitons will transfer to EHP for the radiative recombination process (i.e., lasing spectrum around 395 nm). Consequently, due to the enhancement of the screening Coulomb interaction by the free-carriers from the ionized excitons, all the photoexcited excitons tend to transfer completely to EHP. Therefore, EHP radiative recombination process is dominant in ZnO epilayers with larger tensile strain. On the other hand, it is found that n_{ex} for sample *b* is $\sim 2.12\times 10^{19}/\mathrm{cm}^3$ [i.e., ○ in Fig. 3(b)], which is smaller than the calculated n_{Mott} of the *A*-exciton with ε_{zz} of −0.4%. This indicates that the high n_{Mott} value for ZnO epilayer with compressive strain allows the excitonic state to be sustained and the lasing mechanism is dominated by FE radiative recombination (i.e., lasing at ∼380 nm).

It is noted that the major role of strain in the ZnO epilayers is to determine the mechanism of radiative recombination and the gain of the samples is less dependent on the strain. It is observed from Fig. 1 that the gain of FE radiative recombination is higher than that of the EHP radiative recombination (i.e., sample *b* has lower threshold than sample *a*). This is expected as the gain of excitonic laser action in ZnO is known to be higher than that of EHP lasers.[1,2] Hence, our explanations on the strain dependence of the lasing characteristics in the ZnO epilayers are consistent.

In order to verify our explanation, lasing characteristics of other annealed ZnO samples with various substrates, sample *c*: ZnO (100 nm)/$\mathrm{Zn}_x\mathrm{Si}_{1-x}\mathrm{O}$ (80 nm)/silicon, sample *d*: ZnO (100 nm)/sapphire, and sample *e*: ZnO (100 nm)/quartz, have been investigated. It is found that the residual strain ε_{zz} (lasing peaks excited near threshold) of samples *c*, *d*, and *e* are ∼−0.2%, ∼0.5% and ∼1.3% (∼386 nm, ∼388 nm, and ∼396 nm), respectively. It is estimated that for samples *c* and *d*, the values of n_{ex} are lower than the calculated values of n_{Mott} of the *A*-exciton. The values of n_{ex} (n_{Mott}) for samples *c* and *d* are labeled in Fig. 3 with symbols △ and ▽ (▲ and ▼), respectively. This implied that samples *c* and *d* exhibit excitonic lasing and the corresponding wavelength of lasing peaks (∼386 and ∼388 nm) has supported our claim. On the other hand, sample *e* has value of n_{ex} (◇) higher than the calculated value of n_{Mott} of the *A*-exciton (◆). This indicates that EHP radiative recombination is the dominant mechanism, and this can be justified by the corresponding wavelength of lasing peak (∼396 nm). Furthermore, it is observed that the gain of samples with FE radiative recombination is higher than that with EHP radiative recombination. Hence, the strain dependence of lasing mechanisms in the ZnO epilayers has been explained and verified.

Based on our investigation, we can explain the general observation of FE lasing in nanomaterials.[5,6] This is due to the weak interaction between the ZnO nanomaterials and substrates that results in strain-free nanomaterials. However, ZnO thin films deposited on various substrates (e.g., sapphire, Si, $\mathrm{SiO_2/Si}$, MgO/ZnO/Si, and quartz) under different growth and annealing processes usually experience strong tensile strain or compressive strain so that different emissions from EHP or FE can be observed at RT. In summary, the mechanisms of radiative recombination in ZnO epilayers are investigated. It is demonstrated that the type of strain experienced by the ZnO active layer, resulting in different values of n_{Mott}, plays an important role in determining the recombination process in the ZnO epilayers.

This work was supported by the Agency for Science, Technology and Research of Singapore (Project number: 022-101-0033) and Nippon Sheet Glass Foundation.

[1] Z. K. Tang, G. K. L. Wong, P. Yu, M. Kawasaki, A. Ohtomo, H. Koinuma, and Y. Segawa, Appl. Phys. Lett. **72**, 3270 (1998).
[2] D. M. Bagnall, Y. F. Chen, Z. Zhu, T. Yao, M. Y. Shen, and T. Goto, Appl. Phys. Lett. **73**, 1038 (1998).
[3] H. Cao, Y. G. Zhao, H. C. Ong, S. T. Ho, J. Y. Dai, J. Y. Wu, and R. P. H. Chang, Appl. Phys. Lett. **73**, 3656 (1998).
[4] S. F. Yu, Clement Yuen, S. P. Lau, and H. W. Lee, Appl. Phys. Lett. **84**, 3244 (2004).
[5] H. Cao, J. Y. Xu, E. W. Seeling, and R. P. H. Chang, Appl. Phys. Lett. **76**, 2997 (2000).
[6] M. H. Huang, S. Mao, H. Feick, H. Yan, Y. Wu, H. Kind, E. Weber, R. Russo, and P. Yang, Science **292**, 1897 (2001).
[7] C. F. Klingshirn, *Semiconductor Optics* (Springer, Berlin, 1995), pp. 306–307.
[8] V. Srikant and D. R. Clarke, J. Appl. Phys. **81**, 6357 (1997).
[9] T. Makino, T. Yasuda, Y. Segawa, A. Ohtomo, K. Tamura, M. Kawasaki, and H. Koinuma, Appl. Phys. Lett. **79**, 1282 (2001); Th. Gruber, G. M. Prinz, C. Kirchner, R. Kling, F. Reuss, W. Limmer, and A. Waag, J. Appl. Phys. **96**, 289 (2004).
[10] The Mott density n_{Mott} can be expressed, as in Ref. 7, as $n_{\mathrm{Mott}} = k_B T/2a_B^3|\mathrm{Ry}^*|$, where $a_B(=4\pi\varepsilon_r\varepsilon_0\hbar^2/m_r e^2)$ and $\mathrm{Ry}^*\{=-m_r e^4/[2\hbar^2(4\pi\varepsilon_r\varepsilon_0)^2]\}$ are the Bohr radius and Rydberg energy of excitons, respectively. k_B is the Boltzmann constant and $T=300$ K is room temperature.
[11] A. Shikanai, T. Azuhata, T. Sota, S. Chichibu, A. Kuramata, K. Horino, and S. Nakamura, J. Appl. Phys. **81**, 417 (1997).
[12] The following parameters of wurtzite ZnO are taken from Ref. 13: $m_e^{\parallel}=0.24$; $m_e^{\perp}=0.21$, in units of m_0; $A_1=3.78$, $A_2=-0.44$, $A_3=3.45$, $A_4=-1.63$; $\Delta_1=38$ meV, $\Delta_{\mathrm{SO}}^{\parallel}=-13.59$ meV, $\Delta_{\mathrm{SO}}^{\perp}=-9.15$ meV, $\Delta_2^{\parallel}=\Delta_{\mathrm{SO}}^{\parallel}/3$ meV, $\Delta_2^{\perp}=\Delta_{\mathrm{SO}}^{\perp}/3$ meV; static dielectric constant $\varepsilon_r^{\parallel}=8.49$, $\varepsilon_r^{\perp}=7.40$. $D_3=-1.34$ eV, $D_4=1.0$ eV; $C_{13}=105.1$ GPa, $C_{33}=210.9$ GPa (Ref. 8).
[13] W. R. L. Lambrecht, A. V. Rodina, S. Limpijumnong, B. Segall, and B. K. Meyer, Phys. Rev. B **65**, 075207 (2002).
[14] A. Teke, Ü. Özgür, S. Dogan, X. Gu, H. Morkoç, B. Nemeth, J. Nause, and H. O. Everitt, Phys. Rev. B **70**, 195207 (2004).

Downloaded 24 Jun 2005 to 155.69.4.4. Redistribution subject to AIP license or copyright, see http://apl.aip.org/apl/copyright.jsp